

Microwave Cathode for Air Breathing Electric Propulsion

IEPC-2009-015

*Presented at the 31st International Electric Propulsion Conference,
University of Michigan • Ann Arbor, Michigan • USA
September 20 – 24, 2009*

Kevin D. Diamant*
The Aerospace Corporation, Los Angeles, CA, 90009, USA

Abstract: The feasibility of compensating drag on a small satellite at low orbital altitude using electric propulsion with propellant ingested from the atmosphere is demonstrated using a simple analysis. A microwave powered plasma cathode is described which efficiently produces large electron currents using xenon (10.3 A at 90 mA/W) and argon (5.7 A at 50 mA/W) at 50 V bias and flow rates comparable to thermionic hollow cathodes. This cathode is proposed as a neutralizer on long duration missions in the lower thermosphere.

I. Introduction

THE concept of operationally responsive access to space is leading to increased interest in small, low power, yet capable and flexible spacecraft. Missions include communications and surveillance, both of which benefit from reductions in orbital altitude. By decreasing altitude, smaller, lower power, and less massive instruments can deliver capability similar to that provided by larger satellites in higher orbits. For example, the resolution of Earth imagery is proportional to the ratio of orbital altitude to optical aperture diameter. Today's commercial Earth observing satellites operate at altitudes from 400-800 km and achieve sub-meter resolution. Surveillance from 200 km could improve image resolution by a factor of 2-4, or, for the same resolution, reduce instrument volume/mass by perhaps a factor of 10 or more.

Orbits below approximately 300 km decay rapidly due to atmospheric drag. Drag compensation can be accomplished with on-board propellant,¹⁻³ but for mission durations of several years the propellant mass fraction can become prohibitively large. If propellant is ingested from the ambient atmosphere, payload mass will increase and mission life will become independent of the propellant supply.

Aerodynamic heating precludes orbiting below about 100 km. For orbits above 100 km, the need to achieve appropriate gas density and residence time inside either chemical or electric thrusters requires stagnation of the incoming flow, and subsequent acceleration to greater than orbital velocity (approximately 8 km/s). This will require, and be a new application for, electric propulsion.

Concepts for air breathing electric thrusters have been described by Hruby, et al.⁴ and by Wahl.⁵ Detailed system studies have been presented by Nishiyama^{6,7} and by Di Cara, et al.⁸ In this paper a comparatively crude analysis will be used to demonstrate the feasibility of drag compensation with ingested propellant, and to estimate the required performance of an electric propulsion based solution. Then, progress toward development of a high current, non-thermionic, microwave powered cathode/neutralizer suitable for operation in the oxygen-rich environment of the lower thermosphere will be detailed.

II. Analysis of Drag Compensation

The drag D experienced by a satellite of frontal area (projected area normal to orbital velocity vector) A_f orbiting at velocity v through gas density ρ is:

$$D = \frac{1}{2} \rho v^2 C_D A_f \quad (1)$$

* Research Scientist, Propulsion Science Department, M2-341, kevin.d.diamant@aero.org.

where

$$v = \sqrt{GM_E/(h + R_E)} \quad (2)$$

for a circular orbit, G is the gravitational constant, M_E is the mass of the earth, R_E is the radius of the earth, and h is the orbital altitude. Thrust T is:

$$T = \eta_m \dot{m}_T u_e \quad (3)$$

where \dot{m}_T is the mass flow delivered to the thruster, and η_m (mass utilization efficiency) is the fraction of that flow accelerated to velocity u_e . The mass flow \dot{m}_i entering the atmospheric inlet of area A_i is:

$$\dot{m}_i = \rho v A_i \quad (4)$$

If a mass capture efficiency η_c is defined as:

$$\eta_c = \dot{m}_T / \dot{m}_i \quad (5)$$

Then Eqs. (1) and (3)-(5) can be combined to yield the required exhaust velocity for continuous drag compensation, $T = D$:

$$u_e = v C_D A_f / (2 \eta_m \eta_c A_i) \quad (6)$$

Note that since the incoming flow of atmospheric gas is assumed to be completely stagnated, A_i is included in A_f , and the ratio A_f/A_i has a minimum value of 1. The required power P is:

$$P = T u_e / (2 \eta_T) \quad (7)$$

where η_T is the thruster efficiency. Following Nishiyama,^{6,7} we will assume that the atmospheric inlet consists of a honeycomb of long, slender tubes, such that the rarefied and highly directed incoming flow passes easily, but the thermalized backflow (i.e. flow leaving through the inlet) does not. Balancing the incoming flow against backflow and flow through the thruster yields the following expressions for the neutral number density n_T in the thruster, and for η_c :

$$n_T = n_i (v/v_i) / (a + A_e/A_i) \quad (8)$$

$$\eta_c = (A_e/A_i) / (a + A_e/A_i) \quad (9)$$

where n_i is the free stream number density, v_i is the thermal velocity of the thermalized gas, a is the Clausing factor for escape of thermalized gas through the inlet, and A_e is the open area of the thruster exit. Equations (8) and (9) are for the case of "cold flow" (i.e. no plasma), and are for the purpose of rough estimation.

At this point we will proceed with a sample case in order to demonstrate feasibility, and to inform the design of the microwave cathode. The Jacchia71 (J71) atmospheric density model was selected because it is based on observations of atmospheric drag on satellites.⁹ The J71 model performance (density uncertainty $\sim 15\%$) is comparable to other models that are based on in-situ measurements,^{10,11} however its use for drag calculations is considered to be superior when the same drag coefficient is employed as was used in the model generation (J71 uses $C_D = 2.2$).¹² The satellite is assumed to be small, with a frontal area of 0.5 m^2 and approximately 1 kW available for propulsion. The propellant is accelerated in an electron cyclotron resonance (ECR) ion engine, chosen because it has perhaps the lowest operating pressure of any mature electric thruster technology.¹³ We will assume that reliable thruster operation can be achieved if thruster geometry and gas density are roughly similar to existing ECR thrusters: exhaust open area and neutral density on the order of 10^{-2} m^2 and 10^{18} m^{-3} respectively. Due to the molecular nature and low mass of the atmospheric constituents (mostly O and N₂), we anticipate reduced thruster efficiency and mass utilization efficiency relative to xenon. We will assume, without justification, that $\eta_T = 0.25$ and $\eta_m = 0.50$. For the case of moderate solar activity (exospheric temperature of 1000 K), and at an altitude of 220 km, the orbital velocity, temperature, mean molecular weight, and number density are approximately 7.8 km/s, 900 K, 19 amu, and $5 \times 10^{15} \text{ m}^{-3}$ respectively. At these conditions, the maximum ratio of length to diameter for the inlet tubes such that a molecule traveling at orbital velocity will traverse the tube length before its thermal velocity allows it to traverse the radius (and collide with the wall) is about 16, yielding $a = 0.07$.¹⁴ Taking the ratio of neutral number density in the thruster to that in the atmosphere to be 500 ($n_T = 2.5 \times 10^{18} \text{ m}^{-3}$) leads to an atmospheric inlet area just over half (53%) of the satellite frontal area, and a mass capture efficiency of 35% (a temperature of 300 K was assumed in the calculation of v_i —lower temperatures would increase compression and/or capture efficiency). The required thruster power, thrust, exhaust velocity, accelerating voltage ($V = m u_e^2 / (2q)$, where m is the mean particle mass and q the

elementary charge) and beam current ($J = \eta_r P/V$) are approximately 950 W, 5 mN, 9.2×10^4 m/s, 850 V, and 0.3 A. These values are perhaps most similar to the “ $\mu 20$ ” ECR xenon ion thruster (900 W, 27 mN, 1200 V, 0.5 A).²¹

III. Microwave Cathode

Use of a thermionic hollow cathode, perhaps with a relatively oxygen-tolerant LaB₆ insert,¹⁵ coupled with a small on-board supply of xenon may be an adequate solution to the problem of neutralizing the ion beam from an air-breathing thruster. However, we will assume that, for long duration missions, it is necessary to avoid the use of high operating temperature parts (e.g. cathode heater) exposed to the oxidizing environment. Field emission cathodes operate cold and require no gas, but demonstrated total emission currents are too low for this application, and robustness in non-ultra-high vacuum environments is an open question.^{16,17} A radio frequency (RF) or microwave powered plasma cathode combines the advantages of low temperature operation and tolerance to the widest variety of gases.

RF (inductive)¹⁸⁻²⁰ and microwave (ECR)²¹⁻²⁵ plasma cathodes using xenon and argon have been investigated for electric propulsion applications. Meaningful comparison of the outcomes of these investigations is difficult due to the often nonlinear dependence of electron current on power, pressure, extraction voltage, and anode configuration. Nevertheless, the largest absolute current reported for xenon was 30 A at 1300 W input (23 mA/W),¹⁹ and for argon was 15 A at 1200 W input (12.5 mA/W).²⁰ The latter result was also the most efficient current extraction reported for argon, while that for xenon was 0.50 A at 15 W input (33 mA/W).²¹ In what follows, we will describe a microwave ECR cathode which has produced 10.3 A at 115 W (90 mA/W) on xenon and 5.7 A at 115 W (50 mA/W) on argon.

A. Description of Experiment

The cavity (Figs. 1 and 2) is the same as that studied in Ref. 26, with the exceptions of the addition of a magnet, and the substitution of either sapphire or fused silica for alumina as the vacuum break material. Alumina was replaced due to concerns over porosity. Sapphire (crystalline Al₂O₃) and alumina share very similar electrical properties, while fused silica permitted investigation of the effect of varying the dielectric constant (3.8 vs 9.6 for alumina/sapphire). Our results to date indicate that tuned cavity lengths are larger for fused silica than for sapphire, but extracted currents are nearly the same. All of the data reported here were recorded with sapphire as the vacuum break material.

Microwave power generated by a magnetron at 5.8 GHz was introduced through the coupling antenna (RG401 rigid coaxial cable). The cavity was tuned for maximum power absorption by varying the cavity length (position of sliding short) and the depth of insertion of the coupling antenna. The magnet consists of an array of NdFeB permanent magnets. Figure 3 is a contour plot of magnetic field magnitude in the plasma region. The size of the magnetic field probe did not allow measurements closer than 0.5 cm from the cavity wall. Normalized magnetic field vectors are shown in Fig. 4. The magnitude of the radial magnetic field component varied from approximately 0 to between 20 and 30% of the axial component magnitude. The magnetic field was therefore predominantly axial with monotonically decreasing magnitude in the direction of microwave propagation. This configuration was motivated by the following considerations: microwaves launched parallel to the magnetic field in the direction of decreasing field magnitude encounter the electron cyclotron resonance before encountering the right-hand cutoff,²⁷ presumably increasing the likelihood of power absorption and high plasma density. This configuration also promotes an axial drift of electrons toward the extraction aperture. Since electrons are allowed to escape axially along field lines, ions should not be electrostatically inhibited from drifting radially across field lines to the cavity walls.

The cavity was mounted to a flange (Fig. 5) on a 0.75-m diameter by 1.2-m long turbopumped vacuum chamber. Vacuum pumping speed, as determined by an ionization gauge mounted at the top of the chamber at the same axial location as the cavity, was approximately 5400 l/s on xenon and 7800 l/s on argon (e.g. background pressure of 3×10^{-6} Torr for 1.5 sccm xenon or 9×10^{-6} Torr for 6 sccm argon). Electron current was extracted to a 4-inch (102 mm) diameter, 0.25-inch (6.4 mm) thick, perforated (54% open area) steel anode placed 0.75 inches (19 mm) from the downstream face of the keeper electrode (Fig. 6, “open” anode). The configuration shown in Fig. 7 (“solid” anode) includes a 1.69-inch (4.3 cm) diameter steel plate attached to the downstream face of the anode, blocking the central and six surrounding apertures (open area 43%). The anode was given a positive bias (typically 50 V) relative to the grounded cavity. Plasmas were formed from xenon or argon, primarily for the sake of comparison to other work (referenced in the preceding section). Flow rates were set with thermal mass flow controllers, calibrated by timing the pressure rise in a one liter volume. Cavity pressure was measured with a capacitance manometer. Plasma formation was very reliable and never required the use of any separate ignition device. In all cases it was possible to tune the cavity so that the reflected power was within the measurement uncertainty (10 W). The power absorbed in the plasma was 115 ± 10 W for all of the data presented here.

IV. Results

A number of different extraction aperture and keeper electrode geometries were tested. The best results have been obtained with the keeper geometry shown in Fig. 2, and extraction aperture diameters (dimension D in Fig. 2) of 0.161 (4.1) and 0.228 (5.8) inches (mm). In all cases a current of 0.50 A was extracted to the keeper electrode prior to initiating, and was maintained during, current extraction to the anode. Figure 8 shows extracted currents vs xenon flow rate at 50 V anode bias, including one set without the magnet. The presence of the magnet is shown to increase extracted current by approximately a factor of 3. The extracted currents in Fig. 8 are re-plotted in Fig. 9, where it is apparent that the effect of the solid anode is to increase the cavity pressure during current extraction. Perhaps the solid anode increased the bias imposed at the extraction aperture, providing additional power to the cavity electrons. Cold flow cavity pressures for the data of Figs. 8 and 9 varied from approximately 4 to 80 mTorr. Comparison of Figs. 10 and 11 illustrates a similar effect: increasing anode bias increased current extraction apparently by increasing power dissipation in the cavity, manifested by higher cavity pressure. Again, the solid anode produced a larger effect, presumably by enhancement of the bias impressed at the cavity exit.

Extracted currents with argon are shown in Figs. 12 and 13, where the solid anode again appears to increase cavity pressure during current extraction. Interestingly, the magnet did not increase the extracted current at all flow rates. We should note that at a flow rate of 2 sccm, plasma formation without the magnet was possible, but the keeper would not light at up to 200 V bias, and no current was extracted to the anode. Cold flow pressures for these data varied from approximately 50 to 250 mTorr.

For both gases, the increase in cavity pressure at a given level of current extraction was reduced by removing the magnet. Further work is needed to explain this observation.

V. Discussion

The data permit estimation of a number of properties inside the cavity. With known flow rates, and neutral temperature estimates (several hundred to several thousand degrees K) based on observed pressure increases during current extraction, neutral density for most operating conditions is estimated to be approximately $1\text{--}3 \times 10^{20} \text{ m}^{-3}$ for xenon and $5\text{--}8 \times 10^{20} \text{ m}^{-3}$ for argon. If extracted current is assumed to be limited by ion migration to the cavity walls at the Bohm velocity with an assumed electron temperature T_e of 1 eV, then estimated plasma densities range from 10^{18} to 10^{19} m^{-3} for xenon and 6×10^{17} to $3 \times 10^{18} \text{ m}^{-3}$ for argon (critical density at 5.8 GHz = $4 \times 10^{17} \text{ m}^{-3}$). Ion current limiting is supported by the fact that doubling the electron extraction aperture area did not increase the extracted current for either gas (Figs. 8 and 12). The electron Larmor radius varies (for $T_e = 1$ eV) from approximately 10^{-5} to 3×10^{-4} m, while electron-heavy particle (neutral and ion) elastic collision mean free paths vary from 10^{-3} to 10^{-2} m for both gases, so that ECR heating is possible. The ion Larmor radius for both gases can be smaller than the cavity radius (20 mm) throughout much of the cavity, however ion migration across field lines should be facilitated by charge exchange collisions, for which the mean free paths for both gases are estimated to be a few millimeters.

Measured electron currents from xenon and argon are adequate to neutralize the beam of the notional thruster described in Section II at flow rates that are comparable to or less than those required by today's thermionic hollow cathodes. Current extraction from a nitrogen-oxygen mixture has not been attempted yet, nor has current extraction to a plasma anode. The latter is of concern given the observed influence of anode geometry and bias on extracted current. With regard to the former, it may not be possible at 220 km altitude to compress the incoming atmosphere to densities on the order of 10^{20} m^{-3} . Use of Eq. 8 with assumptions similar to those employed in Section II indicates a maximum compression factor on the order of 10^3 , while a value closer to 10^5 is needed. If xenon is carried on board, then continuous cathode operation for 5 years at a flow rate of 0.5 sccm would require about 8 kg of gas.

VI. Conclusion

A simple analysis has demonstrated the feasibility of compensating drag on a small satellite at an altitude of approximately 200 km with an electric thruster and propellant ingested from the atmosphere. We have described a microwave powered plasma cathode with a coupling antenna that is isolated from the plasma, and which has demonstrated electron current extraction of as much as 10.3 A (90 mA/W) on xenon and 5.7 A (50 mA/W) on argon to an anode in close proximity to the cathode at flow rates similar to those employed by thermionic hollow cathodes. Using a small amount of on-board propellant, this cathode could be a solution to the problem of neutralizing an ion beam on long duration missions in the oxygen-rich thermosphere.

Acknowledgments

This work was supported under The Aerospace Corporation's Independent Research and Development Program. The author thanks Dr. Rostislav Spektor for assistance in producing the magnetic field vector plot (Fig. 4), and Dr. Yevgeny Raitses for insightful discussions.

References

- ¹Fearn, D.G. and Rijm, C., "Low-Cost Remote Sensing from Low Altitude using Ion Propulsion for Drag Compensation," AIAA 2002-3674, 38th Joint Propulsion Conference, Indianapolis, IN, 7-10 July 2002.
- ²St. Rock, B., Blandino, J.J., and Demetriou, M.A., "Propulsion Requirements for Drag-Free Operation of Spacecraft in Low Earth Orbit," Journal of Spacecraft and Rockets, Vol. 43, No. 3, May-June 2006, pp. 594-606.
- ³Bassner, H., Killinger, R., Marx, M., Kukies, R., Aguirre, M., Edwards, C., and Harmann, H.P., "Ion Propulsion for Drag Compensation of GOCE," AIAA 2000-3417, 36th Joint Propulsion Conference, Huntsville, AL, 16-19 July 2000.
- ⁴Hruby, V., Pote, B., Brogan, T., Hohman, K., Szabo, J., and Rostler, P., "Air Breathing Electrically Powered Hall Effect Thruster," U.S. Patent No.: 6,834,492 B2, December 2004.
- ⁵Wahl, E.L., "Air-Breathing Electrostatic Ion Thruster," U.S. Patent Application Publication No.: 2008/0028743 A1, February 2008.
- ⁶Nishiyama, K., "Air Breathing Ion Engine Concept," IAC-03-S.4.02, 54th International Astronautical Congress, Bremen, Germany, 29 September - 3 October 2003.
- ⁷Nishiyama, K., "Air Breathing Ion Engine," ISTS 2004-o-3-05v, International Symposium on Space Technology and Science, 2004.
- ⁸Di Cara, D., Gonzalez del Amo, J., Santovincenzo, A., Dominguez, B.C., Arcioni, M., Caldwell, A., and Roma, I., "RAM Electric Propulsion for Low Earth Orbit Operation: an ESA Study," IEPC 2007-162, 30th International Electric Propulsion Conference, Florence, Italy, 17-20 September, 2007.
- ⁹Jacchia, L.G., "Revised Static Models of the Thermosphere and Exosphere with Empirical Temperature Profiles," Special Report 332, Smithsonian Astrophysical Observatory, Cambridge, MA, 1971.
- ¹⁰Marcos, F.A., "Accuracy of Atmospheric Drag Models at Low Satellite Altitudes," Advanced Space Research, Vol. 10, No. 3-4, pp. (3)417-(3)422, 1990.
- ¹¹Marcos, F.A. and Wise, J.O., "Towards a Golden Age of Satellite Drag," AIAA 2002-0092, 40th Aerospace Sciences Meeting, Reno, NV, 14-17 January 2002.
- ¹²Hedin, A., "Selecting a Model of the Neutral Atmosphere," AIAA 90-0293, 28th Aerospace Sciences Meeting, Reno, NV, 8-11 January 1990.
- ¹³Funaki, I., Kuninaka, H., Toki, K., and Satori, S., "Plasma Diagnostics and Numerical Modeling of a Microwave Ion Engine," AIAA 98-3341, 34th Joint Propulsion Conference, Cleveland, OH, 13-15 July 1998.
- ¹⁴O'Hanlon, J.F., A User's Guide to Vacuum Technology, 3rd Edition, John Wiley and Sons, 2003, p. 36.
- ¹⁵Goebel, D.M., Watkins, R.M., and Jameson, K.K., "LaB₆ Hollow Cathodes for Ion and Hall Thrusters," Journal of Propulsion and Power, Vol. 23, No. 3, May-June 2007.
- ¹⁶Micropulsion for Small Spacecraft, Edited by M.M. Micci and A.D. Ketsdever, Progress in Astronautics and Aeronautics, Volume 187, Chapter 11, 2000.
- ¹⁷Deline, C.A., Goldberg, H.R., Morris, D.P., Ramos, R.A., and Gilchrist, B.E., "Field Emission Cathodes used in the FEGI Get Away Special Shuttle Mission," AIAA 2004-3498, 40th Joint Propulsion Conference, Fort Lauderdale, FL, 11-14 July 2004.
- ¹⁸Godyak, V., Raitses, Y., and Fisch, N.J., "RF Plasma Cathode-Neutralizer for Space Applications," IEPC 2007-266, 30th International Electric Propulsion Conference, Florence, Italy, 17-20 September 2007.
- ¹⁹Longmier, B. and Hershkowitz, N., "Helicon Mode and Xenon Operation with the Nonambipolar Electron Source," AIAA 2007-5308, 43rd Joint Propulsion Conference, Cincinnati, OH, 8-11 July 2007.
- ²⁰Longmier, B., Baalrud, S., and Hershkowitz, N., "Nonambipolar Electron Source," Review of Scientific Instruments 77, 113504 (2006).
- ²¹Kuninaka, H. and Nishiyama, K., "Development of 20 cm Diameter Microwave Discharge Ion Engine μ 20," AIAA 2003-5011, 39th Joint Propulsion Conference, Huntsville, AL, 20-23 July 2003.
- ²²Kamhawi, H., Foster, J.E., and Patterson, M.J., "Operation of a Microwave Electron Cyclotron Resonance Cathode," AIAA 2004-3819, 40th Joint Propulsion Conference, Fort Lauderdale, FL, 11-14 July 2004.
- ²³Edgar, M.C. and Bilen, S.G., "Design and Testing of a High Power Electron Cyclotron Resonance Neutralizer," AIAA 2007-5289, 43rd Joint Propulsion Conference, Cincinnati, OH, 8-11 July 2007.
- ²⁴Hidaka, Y., Foster, J.E., Getty, W.D., Gilgenbach, R.M., and Lau, Y.Y., "Performance and Analysis of an Electron Cyclotron Resonance Plasma Cathode," J. Vac. Sci. Technol. A 25(4), July/August 2007, pp. 781-790.
- ²⁵Weatherford, B.R. and Foster, J.E., "Characterization of a Waveguide ECR Plasma Source," AIAA 2008-4535, 44th Joint Propulsion Conference, Hartford, CT, 21-23 July 2008.
- ²⁶Diamant, K.D., "Plasma Measurements in a Resonant Cavity Hollow Cathode," AIAA 2006-5154, 42nd Joint Propulsion Conference, Sacramento, CA, 9-12 July 2006.
- ²⁷Chen, F.F., Introduction to Plasma Physics and Controlled Fusion, 2nd Edition, Plenum Press, New York, 1984, p. 131.

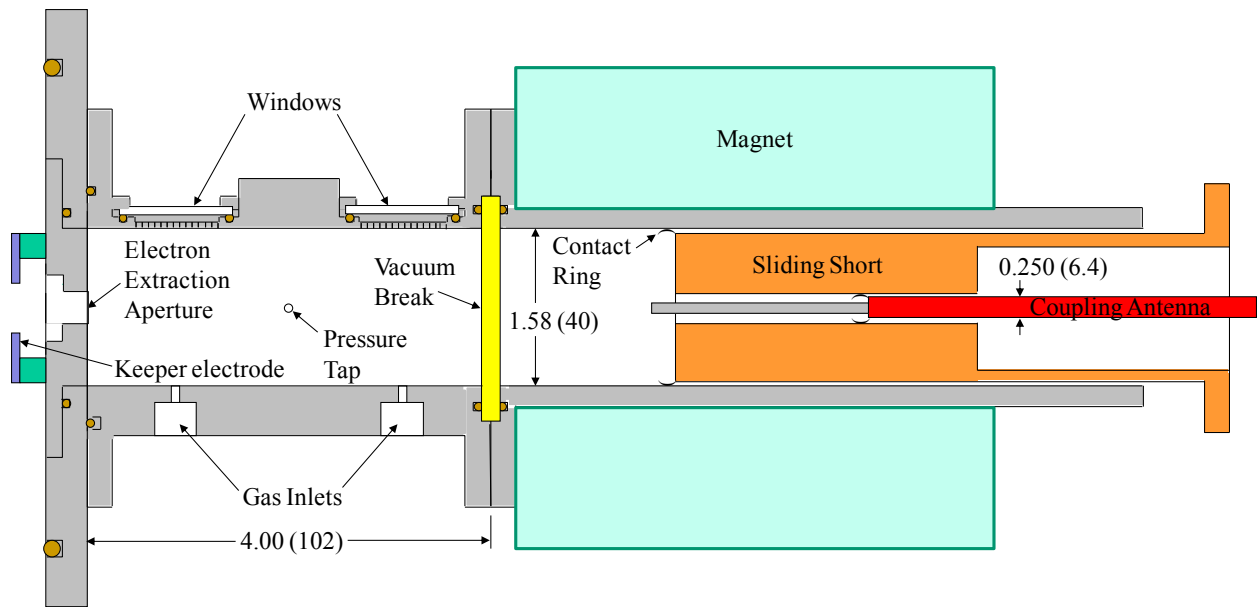


Figure 1. Section view of cavity, dimensions in inches (mm).

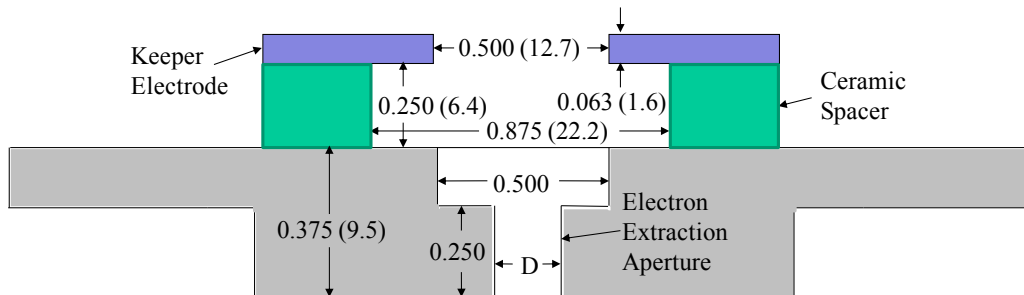


Figure 2. Enlarged section view of extraction aperture and keeper, dimensions in inches (mm).

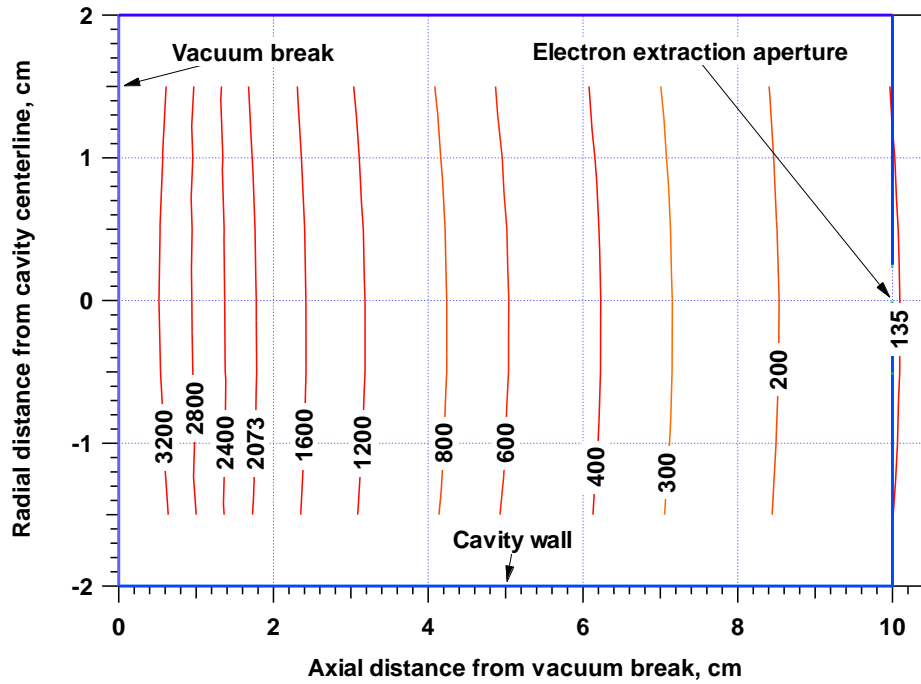


Figure 3. Contour plot of magnetic field magnitude (gauss) in plasma occupied region (outlined in blue). 2073 G contour shows resonant region at 5.8 GHz.

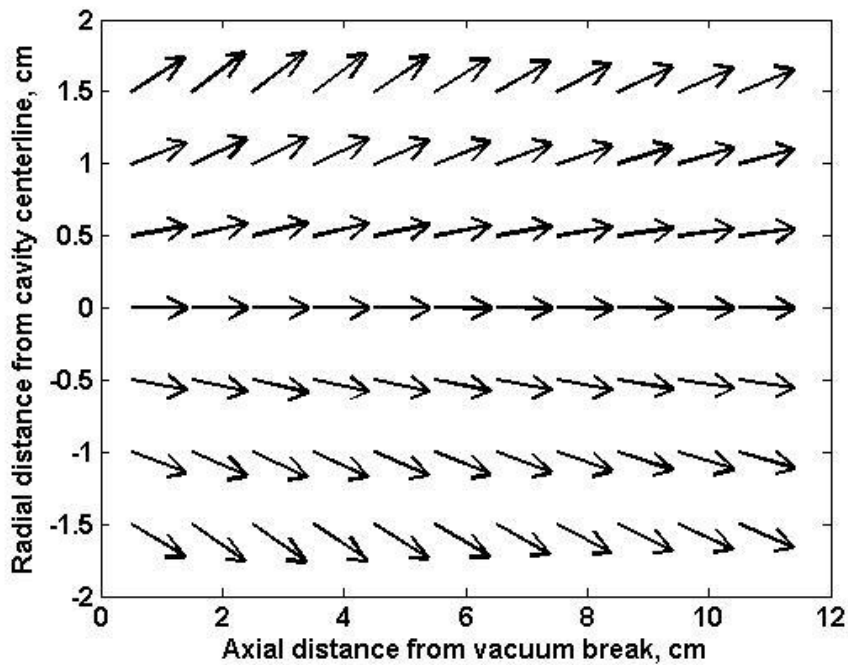


Figure 4. Normalized B field vectors.



Figure 5. Cavity during operation with xenon. Plasma is visible through rectangular windows.

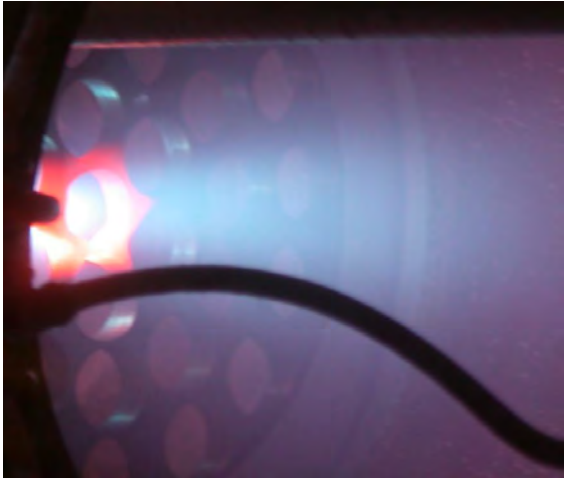


Figure 6. Extraction of approximately 9 A from xenon with 50 V bias on the “open” anode. Cavity aperture is out of view to the left, and is in line with the central anode aperture (glowing red).

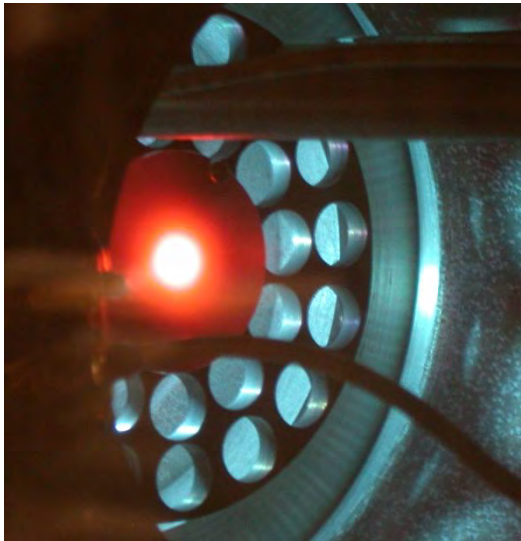


Figure 7. Extraction of approximately 10 A from xenon with 50 V bias on the “solid” anode.

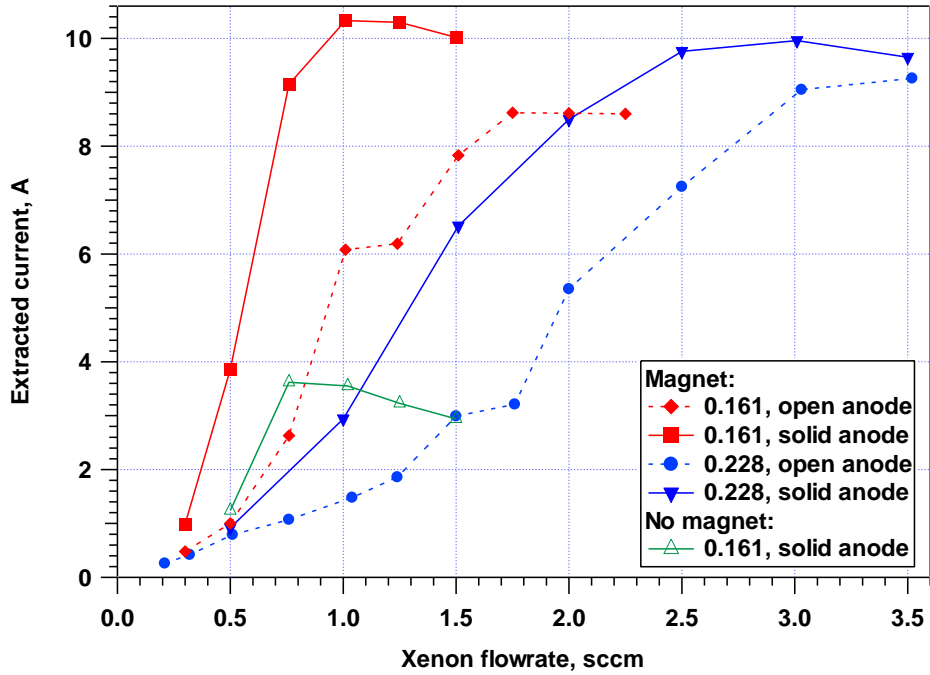


Figure 8. Anode current with 50 V bias, extraction aperture diameters of 0.161 and 0.228-in., with and without the magnet. Solid and open anodes refer to the presence or absence respectively of a 1.69-in. diameter plate attached to the downstream face of the anode.

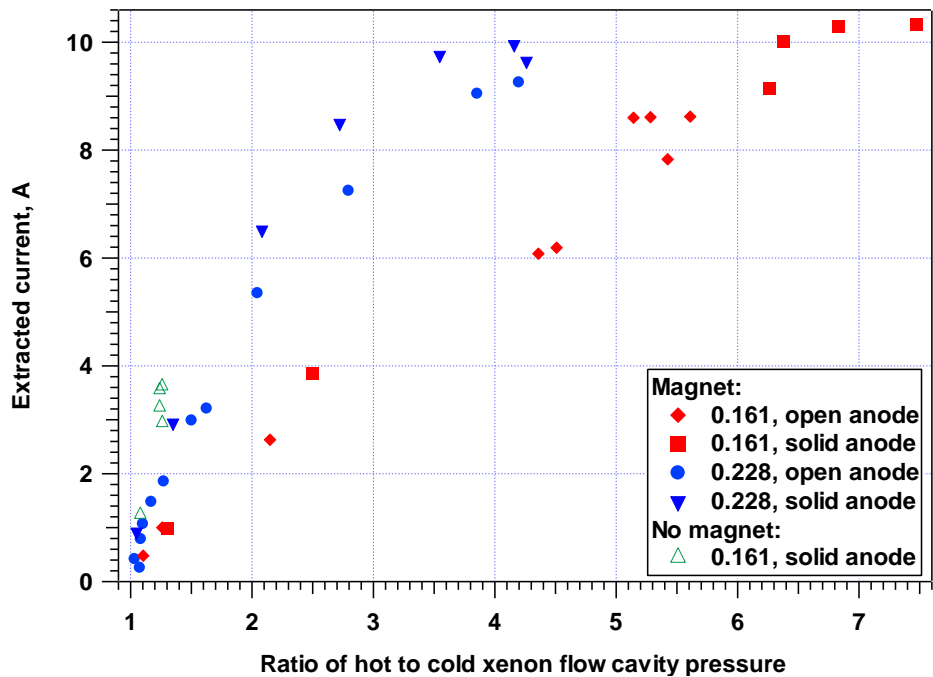


Figure 9. Extracted currents from Fig. 8, plotted against the ratio of cavity pressure during current extraction to cold flow (no plasma) cavity pressure.

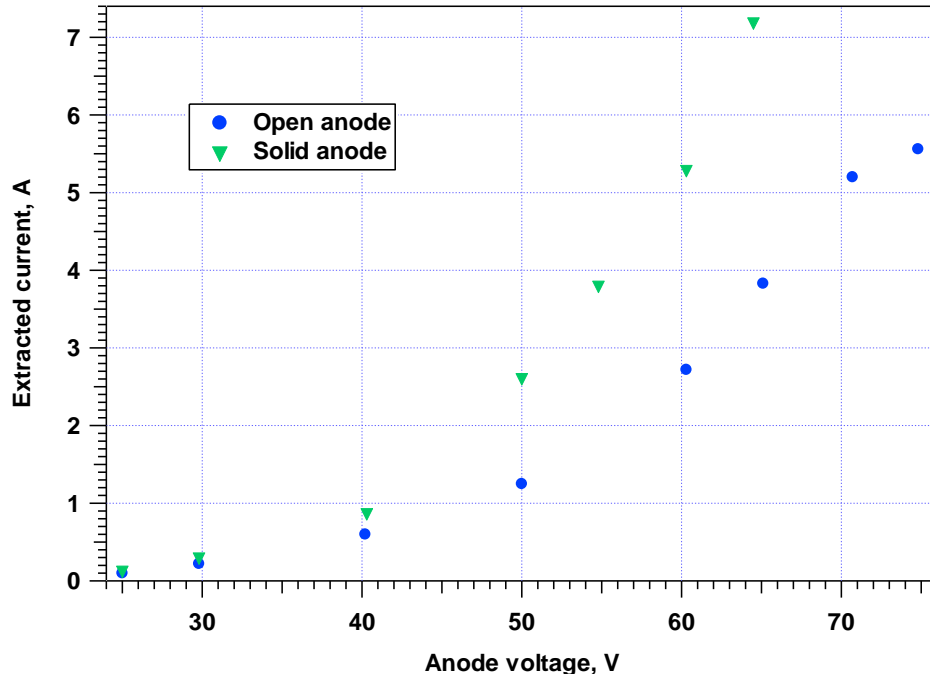


Figure 10. Extracted current at xenon flow rate of 1.0 sccm with 0.228-inch diameter extraction aperture.

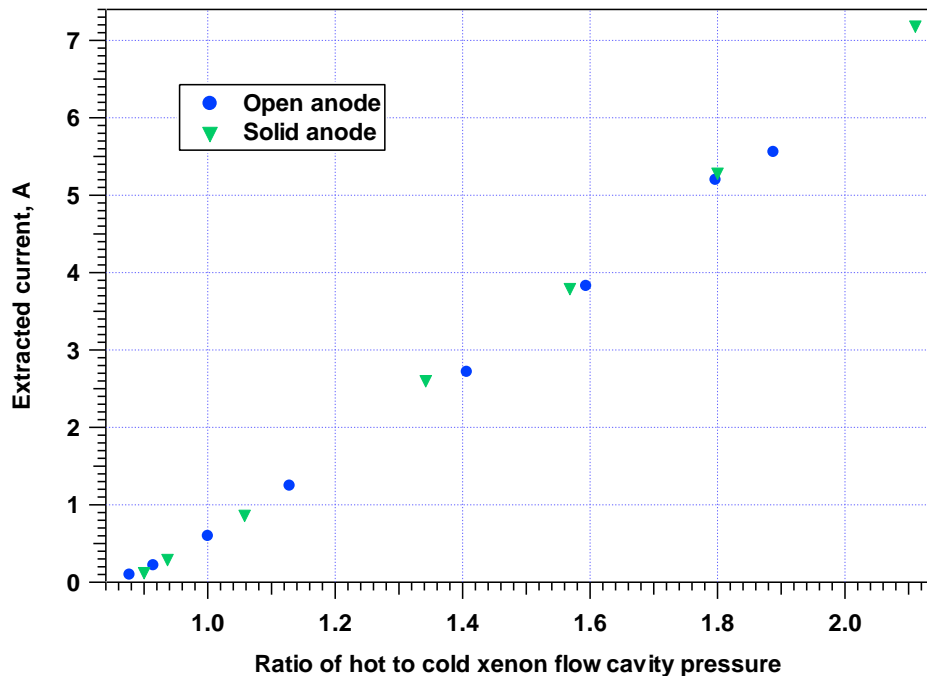


Figure 11. Extracted currents from Fig. 10, plotted against the ratio of cavity pressure during current extraction to cold flow (no plasma) cavity pressure.

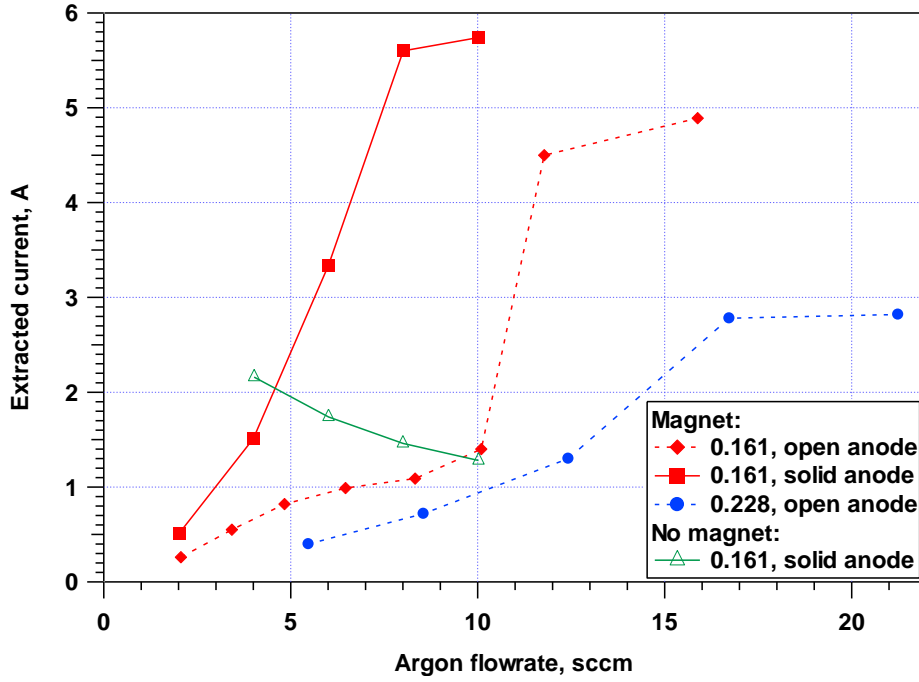


Figure 12. Anode current with 50 V bias, extraction aperture diameters of 0.161 and 0.228-in., with and without the magnet.

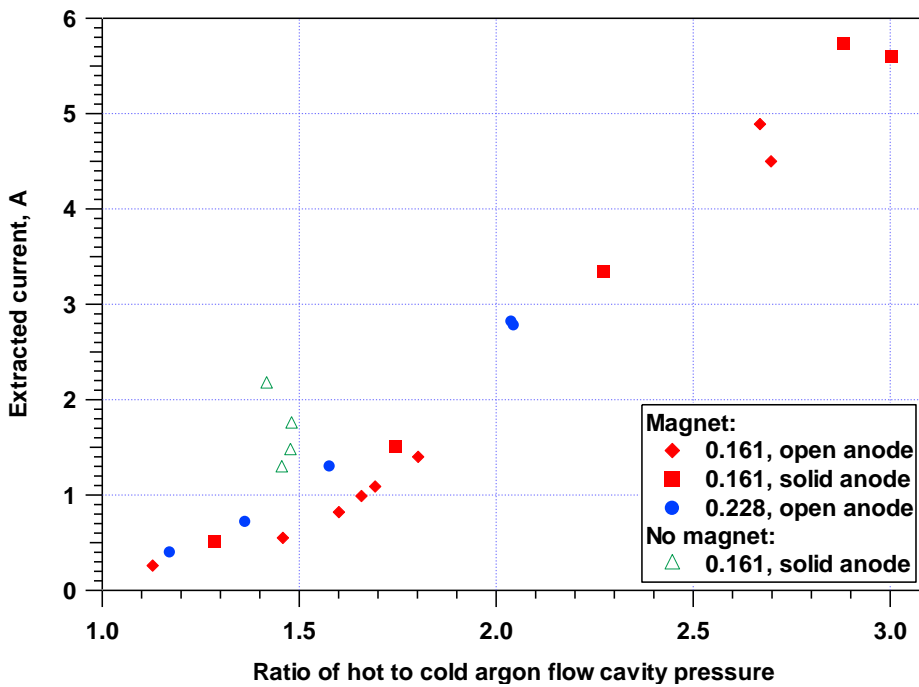


Figure 13. Extracted currents from Fig. 12, plotted against the ratio of cavity pressure during current extraction to cold flow (no plasma) cavity pressure.